Bimetallic cyanido-bridged magnetic materials derived from manganese(III) Schiff-base complexes and pentacyanidonitrosylferrate(II) precursor†

Rodica Ababei,[abcd] Yang-Guang Li,[ab] Olivier Roubeau,[ab] Marguerite Kalisz,[ab] Nicolas Bréfuel,[ab] Claude Coulon,[ab] Etienne Harté,[ab] Xueting Liu,[ab] Corine Mathonière*[cd] and Rodolphe Clérac*[ab]

Received (in Montpellier, France) 19th February 2009, Accepted 9th April 2009
First published as an Advance Article on the web 7th May 2009
DOI: 10.1039/b903399h

Three heterobimetallic $Mn^{III}Fe^{II}$ complexes: $[Mn(5\text{-Br-salpn})(H_2O)]_2[Fe(CN)_5NO]\cdot 2H_2O$ (**1**), $[\{Mn(salen)\}_2Fe(CN)_5NO]\cdot 2H_2O$ (**2**) and $[\{Mn(saltmen)\}_4Fe(CN)_5NO](ClO_4)_2\cdot H_2O\cdot 2CH_3OH$ (**3**), have been synthesized by the reactions of Mn^{III}/Schiff–base (SB) complexes, $[Mn(SB)(H_2O)]^+$, (SB being $salen^{2-}$ = *N*,*N*′-ethylenebis(salicylideneiminato) dianion; 5-Br-$salpn^{2-}$ = *N*,*N*′-1,3-propylenebis(5-bromosalicylideneiminato) dianion or $saltmen^{2-}$ = *N*,*N*′-(1,1,2,2-tetramethylethylene) bis(salicylideneiminato) dianion) with the $[Fe(CN)_5NO]^{2-}$ building block. X-Ray diffraction analyses on single crystals reveal that **1** has a trinuclear molecular structure, **2** displays a two-dimensional (2D) network structure, and **3** possesses a new 2D network of Mn^{III} dinuclear motifs. The magnetic measurements show that the interaction between the Mn^{III} $S = 2$ spins through the [N≡C–Fe–C≡N] bridges is systematically of antiferromagnetic nature: $J/k_B = -0.95(5)$ K and $J/k_B = -1.15(5)$ K for **1** and **2**, respectively, while the direct Mn^{III}–Mn^{III} interaction, in the $\{Mn_2(saltmen)_2\}$ dinuclear units present in **3**, is ferromagnetic with $J/k_B = +1.75(5)$ K. Due to the $S_T = 4$ spin ground state of these dinuclear units and the uniaxial magnetic anisotropy brought by the Mn(III) metal ions, **3** exhibits single-molecule magnet properties. The 400–900 nm optical properties of the three compounds have been also investigated, showing no significant photoactivity unlike in the $Na_2[Fe(CN)_5NO]$ precursor.

Introduction

Molecule-based magnets continue to attract sustained research activities, in particular as a result of the ability of the so-called single-molecule magnets[1] (SMMs) and single-chain magnets[2] (SCMs) to retain their magnetization *i.e.* to exhibit slow relaxation of their magnetization. Due to this magnet-like behavior at the molecular level, these types of compounds are envisioned as qubits for quantum computers and may be the ultimate information storage unit.[3] Numerous SMMs,[1,4] and—comparatively fewer—SCMs[2,5,6] have been synthesized using a number of approaches, though largely relying on serendipitous assembly.[7] In this respect, the cyanide bridging ligand and in particular hexacyanidometalate $[M(CN)_6]^{n-}$ building blocks, that can act as cyanide donor complex-ligands to coordinate other $[M'(L)]^{m+}$ acceptor complexes, allow some rationalization of the synthetic outcome. Indeed, over the last two decades, many cyanide-bridged molecule-based magnetic materials have been isolated with various dimensionalities and magnetic behaviours: classical 3-D magnets in some cases with high-T_c,[8] SMMs,[4b,4f,9] SCMs,[6] spin crossover (SCO) complexes[10] and photomagnetic systems.[11] More specifically, the assembly of hexacyanido-metalate and $[Mn^{III}(SB)]$ (SB = Schiff-base ligands) building blocks have successfully yielded a number of bimetallic polynuclear complexes,[6e,9c,12] 1D[2b,5a,5v,5ah,6e,13] and 2D networks.[8d,14] However, while attention has been mostly focused on the $[Fe(CN)_6]^{3-}$ building block, only few examples have been obtained with other cyanide-containing building blocks.[15]

Only recently, the hexacyanido-metalate precursors have been replaced by $[M(L)(CN)_x]^{n-}$ (x = 1–5) with the substitution of one or more CN groups by the ligand L.[6a–c,6e–h,9a,e,f,16] To some extent, this approach allows to tune the dimensionality and/or topology of the final polynuclear complexes,[17] as well as their magnetic properties.[18] Following this idea we are interested in extending this research subject with the use of $[Fe(CN)_5NO]^{2-}$ building block. Remarkably, this diamagnetic complex has been reported to have a rich photo-chemical

[a] *CNRS, UPR 8641, Centre de Recherche Paul Pascal (CRPP), Equipe "Matériaux Moléculaires Magnétiques", 115 avenue du Dr Albert Schweitzer, F-33600, Pessac, France. E-mail: clerac@crpp-bordeaux.cnrs.fr; Fax: +33 5 56 84 56 00; Tel: +33 5 56 84 56 50*
[b] *Université de Bordeaux, UPR 8641, F-33600, Pessac, France*
[c] *CNRS, UPR 9048, Institut de Chimie de la Matière Condensée de Bordeaux (ICMCB), 87 avenue du Dr. Albert Schweitzer, F-33608, Pessac, France. E-mail: mathon@icmcb-bordeaux.cnrs.fr; Fax: +33 5 40 00 27 61; Tel: +33 5 40 00 26 82*
[d] *Université de Bordeaux, UPR 9048, F-33608, Pessac, France*

† Electronic supplementary information (ESI) available: Additional view of the crystal structures, magnetic data and optical properties of the compounds. CCDC reference numbers 720407–720409. For ESI and crystallographic data in CIF or other electronic format see DOI: 10.1039/b903399h

behavior.[19] Indeed, two long-lived metastable states, SI and SII, can be generated by irradiation at low temperatures at specific wavelengths, and reversible conversion to the ground state can be realized either by irradiation in the red or near-infrared region or by heating over the relaxation temperatures (150 and 200 K, respectively, for SII and SI). An isonitrosyl linkage (*i.e.* Fe^{II}–ON) has been observed in the metastable state SI,[19e] while in the SII metastable state, the NO ligand has a side-on bonded configuration (*i.e.* Fe^{II}–(η^2-NO)).[19e] Such photo-chromic behavior is particularly interesting in the field of photonic materials, *e.g.*, for the development of optical devices for the telecommunication or future optical data storage systems.[20] In bimetallic coordination networks incorporating the photo-sensitive linker $[Fe(CN)_5NO]^{2-}$, one could thus expect the occurrence of new photo-sensitive behaviors. So far, only three examples on such assemblies have been reported,[19b–d] showing that the topology of the coordination network and the environment of the $[Fe(CN)_5NO]^{2-}$ unit is strongly influencing the photo-sensitive properties. Hence, attempts to synthesize new materials based on this building-block appear necessary to investigate further this type of potentially photoactive systems. We report here the synthesis and structures of three new compounds formed by reaction of $[Fe(CN)_5NO]^{2-}$ with $[Mn(SB)]^+$ building blocks: (i) a trinuclear complex, $[Mn(5\text{-Br-salpn})(H_2O)]_2[Fe(CN)_5NO]\cdot 2H_2O$ (**1**); and two 2D coordination networks (ii) $[\{Mn(salen)\}_2Fe(CN)_5NO]\cdot 2H_2O$ (**2**) and (iii) $[\{Mn(saltmen)\}_4Fe(CN)_5NO](ClO_4)_2\cdot H_2O\cdot 2CH_3OH$ (**3**), (with $salen^{2-}$ = *N*,*N*′-ethylenebis(salicylideneiminato) dianion; 5-Br-$salpn^{2-}$ = *N*,*N*′-1,3-propylenebis-(5-bromosalicylideneiminato) dianion and $saltmen^{2-}$ = *N*,*N*′-(1,1,2,2-tetramethylethylene) bis(salicylideneiminato) dianion. Their magnetic properties as well as the effect of irradiation on their physical properties are also analyzed in detail.

Results and discussion

Synthesis

Compounds **1**, **2** and **3** are obtained under similar reaction conditions, which consist in the addition of an aqueous solution of $[Fe(CN)_5NO]^{2-}$ to a methanolic solution of $[Mn(SB)(H_2O)]^+$ in a 1 : 1 stoichiometric ratio. Single-crystals have been obtained by slow evaporation of the resulting solution. The use of three different $[Mn(SB)(H_2O)]^+$ building-blocks (SB being 5-Br-salpn for **1**, salen for **2**, and saltmen for **3**, Scheme 1) produces three cyanido-bridged bimetallic systems.

The IR spectra of the new compounds present all the IR absorptions of the Fe^{II} and Mn^{III} precursors. The peaks around 2150 cm^{-1} assigned to cyanido stretching absorptions are not shifted in energy, but are much less intense than in the $[Fe(CN)_5NO]^{2-}$ precursor suggesting an important modification of the cyanido groups in the final compounds. Furthermore, the strong peak at *ca.* 1910 cm^{-1} is assigned to the NO stretching vibration, which is lower than that found in the sodium salt (1940 cm^{-1}). For **3**, the strong peak centered at 1090 cm^{-1} indicates the presence of ClO_4^- anions. The final compounds present also different stoichiometric Mn : Fe

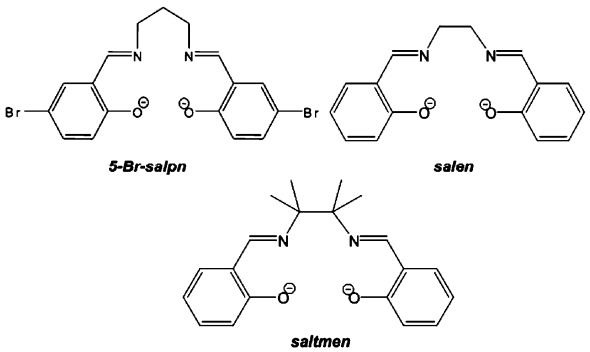

Scheme 1 Schiff base ligands of the Mn(III) complex precursors.

ratios being 2 : 1 for compounds **1** and **2** and 4 : 1 for compound **3**. The 2 : 1 stoichiometry corresponds to the exact compensation of the charges between the $[Fe(CN)_5NO]^{2-}$ anion and the $[Mn(SB)(H_2O)]^+$ cation, and leads to the formation of stable neutral compounds. The excess amount of Mn^{3+} moieties for compound **3** may be explained by the fact that the Mn^{III} derivatives used in this work can be present in solution as a monomer or as an out-of-plane dimer depending on the steric characteristics of the Schiff base ligands.[21] Indeed, for the Mn/saltmen system, a dimeric form has been isolated in the solid state.[22] During the reaction with $[Fe(CN)_5NO]^{2-}$, this dimeric form can be also stabilized in solution, and affects the stoichiometry of the final compound. Finally, as shown below by the structural characterizations of the compounds, **1** is a discrete trinuclear molecule, whereas compounds **2** and **3** form 2D networks. Indeed, the presence of a bulky atom (here, a Br atom) on the phenyl group of the SB ligand for **1** creates steric hindrance on the Mn^{III} cation, and avoids the formation of extended network: previous works show that the association of $[Mn(5\text{-X-salen-like})]^+$ moieties where X is Cl, Br or OMe, with cyanidometalate precursors leads to discrete trinuclear arrangements.[8d,16b,19d]

Crystal structures

Complex **1** crystallizes in the orthorhombic *Pbca* space group and consists of trinuclear units $[Mn(5\text{-Br-salpn})(H_2O)]_2[Fe(CN)_5NO]$. As shown in Fig. 1, two $[Mn(5\text{-Br-salpn})(H_2O)]^+$ fragments are linked by the central $[Fe(CN)_5NO]^{2-}$ moiety.

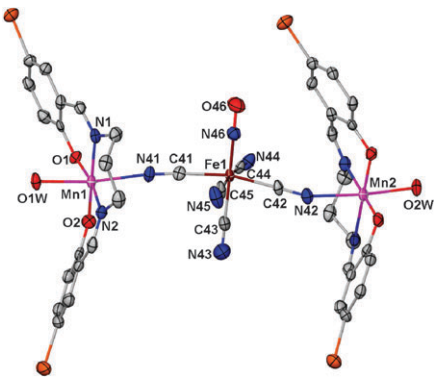

Fig. 1 ORTEP drawing of the basic building unit in complex **1** with the thermal ellipsoids at 50% probability.

Table 1 Selected bond lengths (Å) and bond angles (°) in **1**

Mn1–O2	1.879(4)	Mn(2)–O(4)	1.882(4)
Mn(1)–O(1)	1.900(4)	Mn(2)–O(3)	1.897(4)
Mn(1)–N(1)	2.035(5)	Mn(2)–N(4)	2.040(5)
Mn(1)–N(2)	2.038(5)	Mn(2)–N(3)	2.046(5)
Mn(1)–O(1W)	2.221(4)	Mn(2)–O(2W)	2.184(4)
Mn(1)–N(41)	2.259(5)	Mn(2)–N(42)	2.282(5)
Fe(1)–N(46)	1.650(6)	Fe(1)–C(42)	1.926(6)
Fe(1)–C(45)	1.921(6)	Fe(1)–C(43)	1.937(8)
Fe(1)–C(44)	1.922(6)	Fe(1)–C(41)	1.944(6)
O(2)–Mn(1)–N(41)	92.58(2)	O(4)–Mn(2)–N(42)	89.8(2)
O(1)–Mn(1)–N(41)	95.86(2)	O(3)–Mn(2)–N(42)	89.32(2)
N(1)–Mn(1)–N(41)	85.18(2)	N(4)–Mn(2)–N(42)	89.27(2)
N(2)–Mn(1)–N(41)	92.2(2)	N(3)–Mn(2)–N(42)	86.81(2)
O(1W)–Mn(1)–N(41)	170.1(2)	O(2W)–Mn(2)–N(42)	174.49(2)
N(46)–Fe(1)–C(45)	94.4(2)	N(46)–Fe(1)–C(43)	178.8(3)
N(46)–Fe(1)–C(44)	93.7(3)	N(46)–Fe(1)–C(41)	95.3(3)
N(46)–Fe(1)–C(42)	97.2(3)		

Both Mn^{III} centers are hexa-coordinated by two N and two O atoms of the 5-Br-salpn ligand in the equatorial plane, an axial water ligand and an axial cyanido ligand derived from the $[Fe(CN)_5NO]^{2-}$ moiety, respectively. In the equatorial plane, the average Mn–X bond length is 1.9646(4) Å (X = N or O atom of the 5-Br-salpn ligand; see Table 1). As usually observed for octahedral Mn^{III} ions, the Jahn–Teller distortion leads to elongated axial Mn–O_{water} and Mn–$N_{cyanido}$ (2.221(4) and 2.259(5) Å for the Mn(1) center, 2.184(4) and 2.282(5) Å for the Mn(2) center) bonds. In the $[Fe(CN)_5NO]^{2-}$ fragment, the Fe^{II} center is surrounded by five cyanido ligands and one nitro ligand, exhibiting an octahedral coordination geometry (see Fig. 1). The bond lengths of Fe–C vary from 1.921(7) to 1.943(7) Å, whereas the Fe–N_{nitro} bond length is 1.652(6) Å (see Table 1). These Fe–C/N bond lengths are in good agreement with the reported nitroprusside complexes.[23] In the trinuclear unit, the two $[Mn(5\text{-Br-salpn})(H_2O)]^+$ moieties are linked with $[Fe(CN)_5NO]^{2-}$ fragment *via* the Mn^{III}–N≡C–Fe^{II}–C≡N–Mn^{III} bridge. The bond angles of Mn(1)–N(41)≡C(41) and Mn(2)–N(42)≡C(42) are 151.1(3) and 164.9(3)°, respectively, while the bond angles of N(41)≡C(41)–Fe(1) and N(42)≡C(42)–Fe(1) are 174.6(3) and 176.4(3)°, respectively. Furthermore, the $Mn^{III}\cdots Fe^{II}$ distance is *ca.* 5.228 Å.

Additionally, it is worth mentioning that the NO ligand in such a trinuclear unit is well protected in the "cage" formed by the 5-Br-salpn ligands. The N–O bond length is 1.141(7) Å. The distance between O_{nitro} atom and the center of aromatic ring of the Schiff-base ligands is *ca.* 3.683 Å, indicating the weak intramolecular interactions between O and the aromatic ring (see Fig. S1, ESI†). Interestingly, adjacent trinuclear units are connected into 1-D supramolecular chains along the *a* axis *via* the H-bonding interactions between water ligands and the O atoms derived from the Schiff-base ligand (see Fig. 2(a)). The typical H-bonds are O2W···O1 (2.92(6) Å) and O1W···O3 (2.793(6) Å). These 1-D supramolecular chains are further linked into 2-D supramolecular layers on the [*a* + *c*] plane *via* the H-bonding interactions between water ligands and the cyanido ligands (see Fig. 2(b)). The typical H-bonds are O2W···N44 (2.738(8) Å) and O1W···N45 (2.759(7) Å). In the packing arrangement, these 2-D supramolecular layers are stacked and separated by solvent

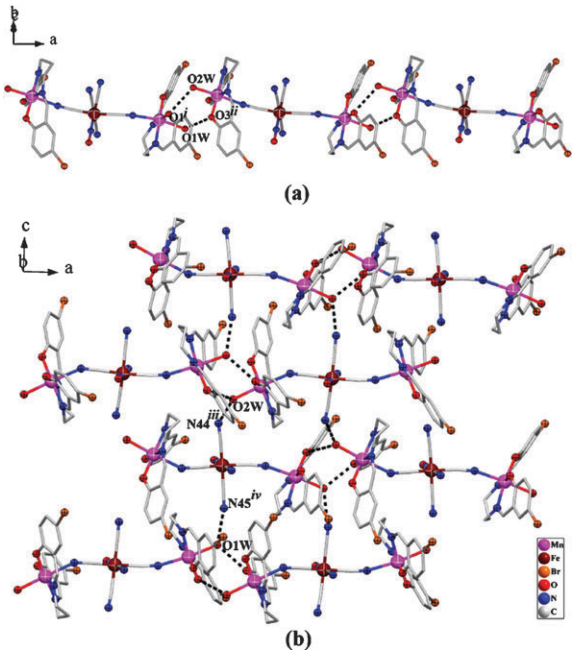

Fig. 2 (a) Ball-and-stick view of the 1-D supramolecular chain in complex **1** based on the H-bonds of O2W···O1^{i} (2.912(6) Å) and O1W···O3^{ii} (2.793(6) Å). (b) 2-D supramolecular layer in complex **1** based on H-bonding interactions of O2W···N44^{iii} (2.738(7) Å) and O1W···O45^{iv} (2.759(7) Å). Symmetry operations are i (1 + *x*, *y*, *z*), ii (−1 + *x*, *y*, *z*), iii (1/2 + *x*, 3/2 − *y*, −*z*), iv (−1/2 + *x*, *y*, 1/2 − *z*).

water molecules. There are no obvious H-bonding interactions between two adjacent supramolecular layers (see Fig. S2, ESI†).

Complex **2** crystallizes in the tetragonal *P*4/*ncc* space group with the chemical formula $[\{Mn(salen)\}_2Fe(CN)_5NO]\cdot 2H_2O$. In complex **2**, the Mn1 site lies on a twofold axis and its salen ligand lies about the same twofold axis. All these Mn centers are hexa-coordinated with two N and two O atoms of the salen ligand in the equatorial plane, and two axial cyanido ligands derived from the $[Fe(CN)_5NO]^{2-}$ moiety (as shown in Fig. 3).

In the equatorial plane, the average Mn–X bond length is 1.936(3) Å (X = N or O atom of the salen ligand; see Table 2). The Jahn–Teller elongation axis is along N(11)–Mn(1)–N(11A) (see Fig. 3), with Mn–$N_{cyanido}$ bond

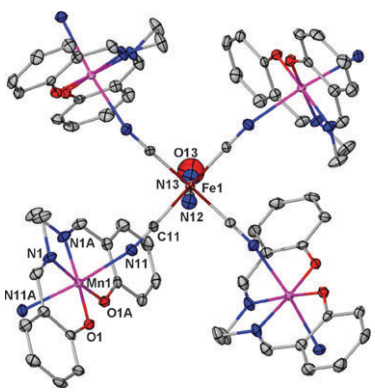

Fig. 3 ORTEP drawing of the basic building units and their connection mode in complex **2** with the thermal ellipsoids at 30% probability. Symmetrical operation: A, −1/2 + *y*, 1/2 + *x*, 1/2 − *z*.

Table 2 Selected bond lengths (Å) and bond angles (°) in **2**

Mn(1)–O(1A)	1.888(3)	Fe(1)–N(13)	1.661(7)
Mn(1)–O(1)	1.888(3)	Fe(1)–C(12)	1.928(8)
Mn(1)–N(1)	1.985(3)	Fe(1)–C(11)	1.938(4)
Mn(1)–N(11)	2.305(4)		
O(1A)–Mn(1)–N(11)	89.79(13)	N(11A)–Mn(1)–N(11)	174.43(18)
O(1)–Mn(1)–N(11)	93.92(12)	N(13)–Fe(1)–C(11)	95.09(12)
N(1)–Mn(1)–N(11)	89.81(14)	N(13)–Fe(1)–C(12)	180.0 (1)
N(1A)–Mn(1)–N(11)	85.96(14)		

Symmetry transformations used to generate equivalent atoms: A: $y - 1/2$, $x + 1/2$, $-z + 1/2$.

length of 2.305(4) Å. This elongation axis is slightly bent with an angle of 174.43(2)°. In the $[Fe(CN)_5NO]^{2-}$ fragment, the Fe1 center lies at a site with fourfold symmetry. Such a Fe^{II} center is surrounded by five cyanido ligands and one nitro ligand, exhibiting an octahedral coordination geometry. The Fe–C bond lengths vary from 1.928(8) to 1.938(4) Å, whereas the Fe–N_{nitro} bond length is 1.661(7) Å (see Table 2). The Fe–C/N bond lengths are similar to those in complex **1**. With these coordination spheres, the $[Mn(salen)]^+$ and $[Fe(CN)_5NO]^{2-}$ fragments are linked into 2-D networks (see Fig. 4) *via* the Mn^{III}–N≡C–Fe^{II} bridges. In such a 2-D network, each $[Fe(CN)_5NO]^{2-}$ unit is surrounded by four $[Mn(salen)]^+$ moieties, while each $[Mn(salen)]^+$ unit is connected by two $[Fe(CN)_5NO]^{2-}$ fragments, forming a (4,4)-net. The bond angles of Mn(1)–N(11)≡C(11) and N(11)≡C(11)–Fe(1) are 160.96(13) and 178.76(13)°, respectively. The $Mn^{III}\cdots Fe^{II}$ distance is *ca.* 5.309 Å. It is also noteworthy that each NO ligand in complex **2** is well surrounded by four aromatic rings derived from four salen ligands and one CN ligand from the adjacent layer (see Fig. S3, ESI†). The distance between O_{nitro} atom and the center of the aromatic ring is *ca.* 4.228 Å, whereas the distance between O_{nitro} and N of the cyanido ligands is *ca.* 2.768 Å, suggesting extensive weak intra- and inter-molecular interactions, which could stabilize the NO ligand in complex **2**.

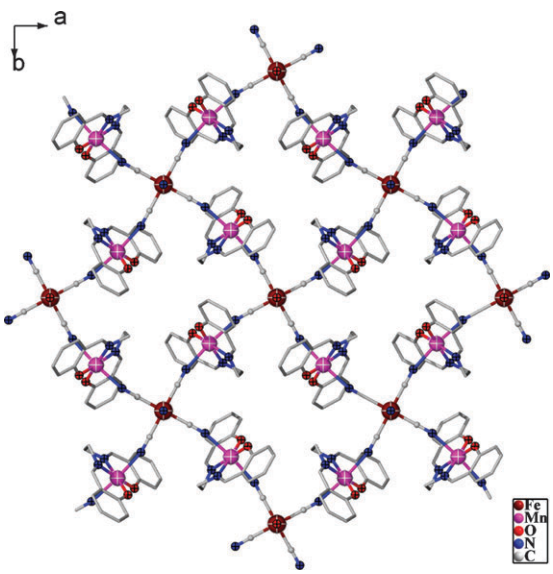

Fig. 4 Ball-and-stick view of the 2-D layer in complex **2**.

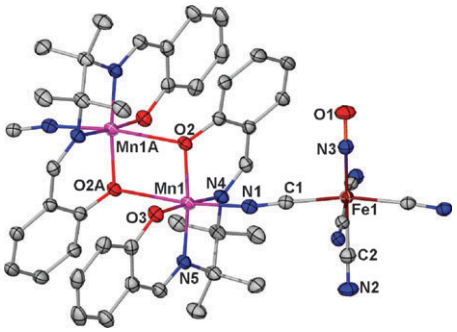

Fig. 5 ORTEP drawing of the basic building units and their connection mode in complex **3** with the thermal ellipsoids at 30% probability.

In the packing arrangement, the adjacent layers exhibit weak π···π interactions of the aromatic rings derived from the salen ligands of different layers (see Fig. S4, ESI†). The shortest distance between two aromatic planes is *ca.* 3.75 Å. The solvent water molecules reside in between the 2-D networks.

Complex **3** crystallizes in the tetragonal *I*4/*m* space group and consists of the cationic 2-D network $[\{Mn(saltmen)\}_4Fe(CN)_5NO]^{2+}$, ClO_4^- counter anions and disordered solvent methanol and water molecules. The cationic layer of $[\{Mn(saltmen)\}_4Fe(CN)_5NO]^{2+}$ includes two basic building units, that is, the dimeric $[Mn^{III}_2(saltmen)_2]^{2+}$ cation and $[Fe^{II}(CN)_5NO]^{2-}$ anion (as shown in Fig. 5).

In the dimeric $\{Mn^{III}_2\}$ units, both Mn^{III} centers are surrounded by two N and two O atoms of the saltmen ligand in the equatorial plane, one axial N atom derived from $[Fe^{II}(CN)_5NO]^{2-}$ unit and one axial O atom derived from the neighboring $[Mn^{III}(saltmen)]^+$ moiety. In the equatorial plane, the average Mn–X bond length is 1.931(4) Å (X = N or O atom of the saltmen ligand; see Table 3). As usually observed for octahedral Mn^{III} ions, the Jahn–Teller distortion leads to elongated axial Mn–$N_{cyanido}$ and Mn–$O_{saltmen}$ (2.246(4) and 2.583(4) Å) bonds. The $Mn^{III}\cdots Mn^{III}$ distance in the dimeric moiety is 3.451(4) Å, while the Mn–O–Mn angle is 99.63(4)° (see Table 3). It is noteworthy that the elongated axial bond length Mn–$O_{saltmen}$ of complex **3** is longer than those in the $[Mn_2(saltmen)_2(H_2O)_2](ClO_4)_2$ precursors.[22]

In the $[Fe(CN)_5NO]^{2-}$ fragment, the Fe1 center lies at a site with fourfold symmetry. This Fe^{II} center is hexa-coordinated with five cyanido ligands and one nitro ligand. The Fe–C bond lengths are in the range of 1.931(4) ~ 1.952(1) Å, whereas the

Table 3 Selected bond lengths (Å) and bond angles (°) in **3**

Mn(1)–O(3)	1.872(3)	Mn(1)–N(5)	1.973(4)
Mn(1)–O(2)	1.898(3)	Fe(1)–C(1)	1.931(4)
Mn(1)–O(2A)	2.583(4)	Fe(1)–C(2)	1.952(1)
Mn(1)–N(1)	2.246(4)	Fe(1)–N(3)	1.662(8)
Mn(1)–N(4)	1.984(4)		
O(3)–Mn(1)–N(1)	92.78(14)	O(2A)–Mn(1)–N(1)	171.03(4)
O(2)–Mn(1)–N(1)	91.78(13)	N(3)–Fe(1)–C(1)	95.69(13)
N(5)–Mn(1)–N(1)	100.18(14)		
N(4)–Mn(1)–N(1)	88.16(14)	N(3)–Fe(1)–C(2)	180.0 (1)

Symmetry transformations used to generate equivalent atoms: A: $1/2 - x$, $1/2 - y$, $1/2 - z$.

Fe–N_{nitro} bond length is 1.662(8) Å (see Table 3). The Fe–C/N bond lengths are similar to those in complexes **1** and **2**. In a similar arrangement as in **2**, the $[Mn_2(saltmen)_2]^{2+}$ and $[Fe(CN)_5NO]^{2-}$ units are connected into a 2-D network (see Fig. 6) *via* the Mn^{III}–N≡C–Fe^{II} bridges, with each $[Fe(CN)_5NO]^{2-}$ unit being surrounded by four dimeric $[Mn_2(saltmen)_2]^{2+}$ moieties, and each $[Mn_2(saltmen)_2]^{2+}$ fragment being connected by two $[Fe(CN)_5NO]^{2-}$ units, forming a (4,4)-net. The bond angles Mn(1)–N(1)≡C(1) and N(1)≡C(1)–Fe(1) are 157.43(13) and 176.15(13)°, respectively, and the $Mn^{III}\cdots Fe^{II}$ distance is *ca.* 5.217 Å. In such a 2-D network, NO ligands are also well enclosed in the "cage" formed by four aromatic rings of saltmen ligands (see Fig. S5, ESI†). The distance between O_{nitro} atom and every center of the aromatic ring is *ca.* 3.965 Å, indicating the possible weak intra-molecular interactions between NO and the aromatic ring group. In the packing arrangement, the adjacent 2-D networks are well separated by the ClO_4^- counter anions, solvent methanol and water molecules (see Fig. S6). The shortest Mn···Mn distance between two planes is *ca.* 11.77 Å.

To conclude this description of the crystal structures, we have summarized the detailed crystal data and structure refinement for **1–3** in Table 4.

Magnetic properties

The magnetic properties of **1**, **2** and **3** have been measured using dc and ac techniques. The dc magnetic susceptibilities measured on polycrystalline samples of **1** and **2** (in the temperature range of 1.8–300 K under an applied magnetic field of 1000 Oe) are shown in Fig. 7 as a χT *vs.* T plot. The χT product gradually decreases from 6.0 and 6.2 cm^3 K mol^{-1} at 300 K to reach a minimum value of 0.41 and 2.90 cm^3 K mol^{-1} at 1.8 K for **1** and **2**, respectively. The room temperature χT values are in good agreement with the expected Curie constant for two isolated Mn^{III} $S = 2$ spins ($C = 6$ cm^3 K mol^{-1}) and a g value very close to 2. The observed thermal behavior is typical of a paramagnetic material that possesses antiferromagnetic interactions between spin carriers *i.e.* $[Mn(SB)]^+$ units. In both **1** and **2**, these antiferromagnetic interactions are most likely mediated by diamagnetic [NC–$(Fe(CN)_3NO)$–CN] links that bridge the $[Mn(SB)]^+$ moieties.

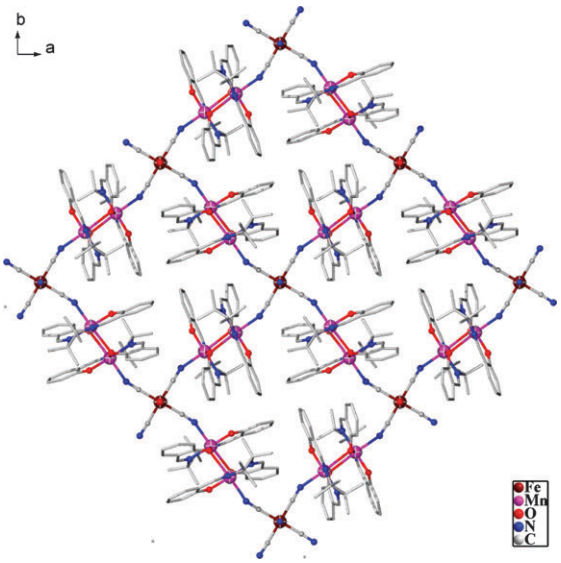

Fig. 6 Ball-and-stick view of the 2-D layer in complex **3**.

In order to estimate the magnitude of these interactions, the experimental data of **1** and **2** have been modeled using as a first approximation, isotropic Heisenberg Hamiltonians for an $S_{Mn} = 2$ dimer (eqn (1)) and a two-dimensional square lattice of $S_{Mn} = 2$ spins (eqn (2)), respectively, according to the obtained crystal structures (*vide supra*).

$$H = -2J\vec{S}_{Mn1}\bullet J\vec{S}_{Mn2} \quad (1)$$

$$H = -2J\sum_{i,j}\vec{S}_{i,j}\left(\vec{S}_{i+1,j} + \vec{S}_{i,j+1}\right) \quad (2)$$

The respective analytical expressions of the magnetic susceptibility can be obtained from the refs. 24 and 25. As shown in Fig. 7, these theoretical approaches have been able to reproduced well the experimental data using the following sets of parameters: $J/k_B = -0.95(5)$ K with $g = 2.0$ for **1** and $J/k_B = -1.15(5)$ K with $g = 2.07$ for **2**. As expected, the two values of the magnetic interaction between Mn^{III} spins through the diamagnetic [NC–$(Fe(CN)_3NO)$–CN] links are similar and close to the reported ones.[19d] Nevertheless it is worth mentioning that these interactions are certainly slightly overestimated by these modeling approaches as their estimation also contains phenomenologically the effects of the magnetic anisotropy brought by the Mn^{III} metal ions. Attempts to simulate the experimental data for **1** including both effects failed and lead to multiple solutions and thus overparametrization of the simulation.

The dc magnetic susceptibility measured at 1000 Oe on a polycrystalline sample of **3** is shown in Fig. 8 as a χT *vs.* T plot. The χT product gradually increases from 12.2 cm^3 K mol^{-1} at 300 K to reach a maximum value of 19.6 cm^3 K mol^{-1} at 4.8 K before decreasing down to 18.7 cm^3 K mol^{-1} at 1.8 K. The room temperature χT value is in good agreement with the expected Curie constant for four isolated Mn^{III} $S = 2$ spins ($C = 12$ cm^3 K mol^{-1}) and a g factor very close to 2. The observed thermal behavior is typical of a paramagnetic material that possesses dominant ferromagnetic interactions between spin carriers *i.e.* $[Mn(saltmen)]^+$ units. As shown in both compounds **1** and **2**, the diamagnetic [N–$(Fe(CN)_3NO)$–CN] link is clearly mediating significant antiferromagnetic interactions between the $[Mn(SB)]^+$ moieties. Therefore the observed ferromagnetic interactions are necessarily present in the dinuclear $[Mn_2(saltmen)_2]^{2+}$ units between Mn^{III} through the bisphenolate bridge as already described in related series of dinuclear complexes.[22,26] On the other hand, the decrease of the χT product below 4.8 K is associated (i) to the presence of antiferromagnetic interactions between $S = 2$ $[Mn(saltmen)]^+$ moieties possibly through the diamagnetic [NC–$(Fe(CN)_3NO)$–CN] link and/or (ii) to the magnetic anisotropy brought by the Mn^{III} metal ions.

Considering the 2D network of magnetic interactions and also that ferromagnetic interactions are dominating, an estimation of the exchange couplings has been performed simulating the thermal dependence of the magnetic

Table 4 Crystal data and structure refinement parameters for compounds **1–3**

Compounds	**1**	**2**	**3**
Formula	$C_{39}H_{36}Br_4FeMn_2N_{10}O_9$	$C_{37}H_{28}FeMn_2N_{10}O_6$	$C_{87}H_{98}Cl_2FeMn_4N_{14}O_{20}$
M/g mol^{-1}	1274.15	874.42	2006.30
λ/Å	0.71073	0.71073	0.77490
Crystal size/mm	0.28 × 0.26 × 0.24	0.28 × 0.26 × 0.23	0.18 × 0.16 × 0.02
Crystal system	Orthorhombic	Tetragonal	Tetragonal
Space group	*Pbca*	*P*4/*ncc*	*I*4/*m*
a/Å	14.851(3)	14.751(2)	18.5154(8)
b/Å	23.826(5)	14.751(2)	18.5154(8)
c/Å	28.135(6)	17.063(3)	27.4984(13)
V/Å^3	9955(3)	3713.1(11)	9427.0(7)
Z	8	4	4
D_c/g cm^{-3}	1.700	1.564	1.414
μ/mm^{-1}	4.057	1.116	0.994
Reflections collected/unique	16519/8716	5480/1635	26410/4752
R_{int}	0.039	0.0363	0.0781
Restraints/parameters	12/606	18/137	194/367
Final R indices [$I > 2\sigma(I)$]: R_1, wR_2	0.0505, 0.1419	0.0496, 0.1318	0.0699, 0.2085
R indices (all data): R_1, wR_2	0.0754, 0.1514	0.0564, 0.1390	0.0855, 0.2284
GOF on F^2	1.17	0.969	1.062
$\Delta\rho_{max/min}$/e Å^{-3}	1.568/−1.274	3.35/−0.776	1.652/−0.787

$R_1 = \sum||F_o| - |F_c||/\sum|F_o|$ and w$R_2 = [\sum w(F_o^2 - F_c^2)^2/\sum w(F_o^2)^2]^{1/2}$.

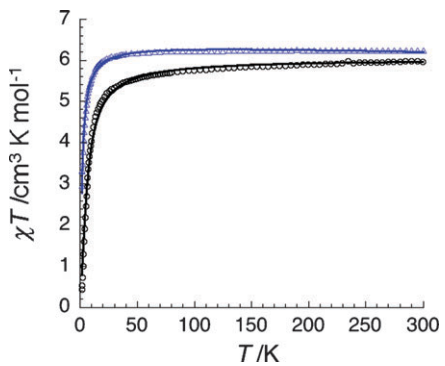

Fig. 7 Temperature dependence of the χT product at 1000 Oe (with $\chi = M/H$ normalized per mol) for **1** (black) and **2** (blue). The solid lines are the best fit obtained with the two models described in the text.

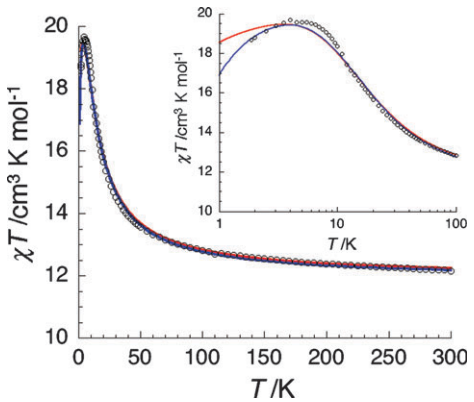

Fig. 8 Temperature dependence of the χT product at 1000 Oe (with $\chi = M/H$ normalized per mol) for **3** (○). Inset: expansion view of the main figure below 100 K in semi-logarithmic plot. The solid lines are the best fits obtained with the models described in the text.

susceptibility from the isotropic Heisenberg Hamiltonian given by eqn (1). Using this model and the deduced susceptibility (χ_{Mn2}) for an $S = 2$ Mn^{III} dimer,[24] an acceptable simulation of the χT *vs.* T experimental data (shown in Fig. 8 by the red solid line) has been obtained introducing inter-dimer Mn$^{III}\cdots$Mn^{III} interactions in mean-field approximation (J').[27] The best set of parameters is $J/k_B = +1.9(1)$ K, $zJ'/k_B = -0.003(1)$ K and $g = 2.00(2)$. This model leads to a very small value of J' that corresponds to a Mn$^{III}\cdots$Mn^{III} of −0.002 K.[28] This value is clearly not compatible with the magnetic interaction estimated in **1** and **2** and expected through the diamagnetic [NC–(Fe(CN)$_3$NO)–CN] link. Therefore, this approach likely underestimates the real value of interaction as J is probably corrected by weaker antiferromagnetic interactions through the $[Fe(CN)_5NO]^{2-}$ unit. The obtained J parameter is thus certainly a minimum estimation of its real value even if +1.9 K is compatible with previously reported values in similar dinuclear $[Mn_2(SB)_2]^{2+}$ complexes possessing an $S_T = 4$ spin ground state.[22,26] This first approach to fit the experimental data leads to the conclusion that the decrease of the χT product below 4.8 K is probably associated mainly with the magnetic anisotropy brought by the Mn^{III} metal ions. Therefore an alternative model has been used to estimate this anisotropy considering (i) the Hamiltonian given in eqn (3) and (ii) the approximation that the Mn$^{III}\cdots$Mn^{III} interaction contains phenomenologically the intra- and inter- $[Mn_2(saltmen)_2]^{2+}$ complex interactions.

$$H = -2J\vec{S}_{Mn1}\bullet\vec{S}_{Mn2} + D_{Mn}(S^2_{z,Mn1} + S^2_{z,Mn2}) \qquad (3)$$

The magnetic susceptibility has been numerically calculated using the MAGPACK program,[29] and compared with the experimental data. The best simulation shown in solid blue line in Fig. 8 corresponds to $J/k_B = +1.9(1)$ K, $D_{Mn}/k_B = -1.0(1)$ K and $g = 2.00(2)$. As expected the magnetic interaction, J, has the same value as in the first modeling approach. On the other hand, the D_{Mn} parameter estimated at −1 K is relatively small in comparison to the reported values on similar complexes that range typically from −3 to −5 K.[22,26] This result seems to indicate that the role of the magnetic

interaction between $[Mn_2(saltmen)_2]^{2+}$ might also preclude a good estimation of the magnetic anisotropy of the system.

As a complete theoretical model taking into account both the 2D topology of the magnetic interactions and the presence of magnetic anisotropy is not available to estimate the magnetic susceptibility of this system, it has not been possible to further analyze these experimental data. Therefore the obtained values of the different magnetic parameters given above must be taken with caution.

In order to probe the presence of slow dynamics of the magnetization in **3** and thus the presence of SMM or SMM-like behavior, ac susceptibility measurements have been performed. The measurements were made in zero dc-field at 100 and 1000 Hz and at temperatures between 1.8 and 7 K (Fig. S7, ESI†). Compound **3** displays frequency-dependent out-of-phase signals suggesting that this compound exhibits slow relaxation of its magnetization. Unfortunately due to our available ranges of ac frequency (up to 1500 Hz) and temperature (down to 1.8 K) with our equipment, the characteristic relaxation time (τ) of the system can be followed in temperature only with ac frequency above 1000 Hz (at 1.8 K, $\tau = 2.4 \times 10^{-4}$ s). In other words the relaxation time of the system in zero dc-field is too fast for our ac technique to be studied accurately in temperature. Therefore in order to reduce a possible fast zero-field relaxation usually induced by quantum tunneling effects in SMMs, a small dc field between 0 and 5000 Oe has been applied at 1.8 K (Fig. 9 and S8, ESI†). The relaxation is dramatically slowed down from 665 Hz in zero dc-field to *ca.* 2.5 Hz in an optimum dc field of about 1800 Oe (Fig. 10) confirming the presence of fast zero-field relaxation as already observed in related $S_T = 4$ dinuclear $[Mn_2(SB)_2]^{2+}$ complexes.[22,26]

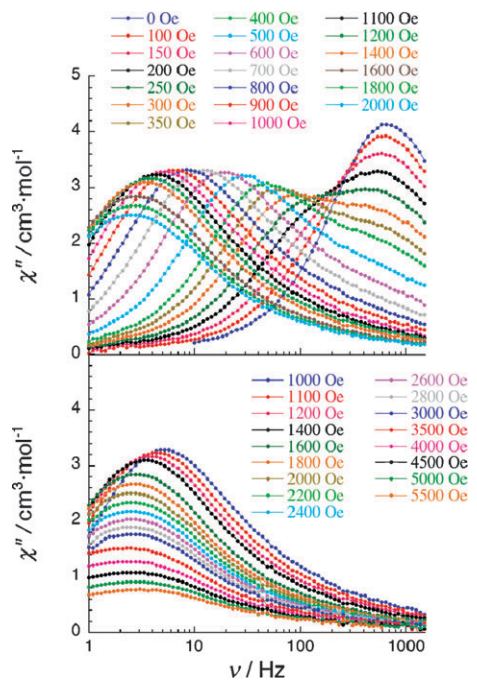

Fig. 9 Frequency dependence of the out-of-phase component of the ac susceptibility for **3** as a function of the ac frequency between 1 and 1500 Hz at 1.8 K under dc-fields.

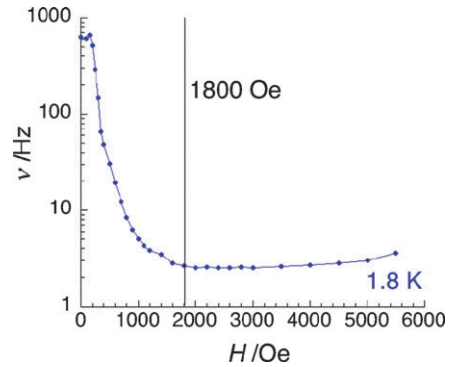

Fig. 10 Field dependence of the characteristic frequency at 1.8 K for **3** deduced from Fig. 9.

Hence to estimate the temperature dependence of the relaxation time, ac data were collected at 1800 Oe (Fig. 11 and S9, ESI†). Under 1800 Oe, a clear maximum is now detected on the χ'' *vs.* T and χ'' *vs.* ν data (Fig. 11 and S9, ESI†) allowing the determination of the relaxation time of **3** in a relatively large temperature domain.

As expected for SMMs, the deduced relaxation time follows a thermally-activated (Arrhenius) behavior (Fig. 12): $\tau = \tau_0 \exp(\Delta_{eff}/k_B T)$ with $\tau_0 = 3 \times 10^{-8}$ s and an energy gap $\Delta_{eff}/k_B = 26.6$ K. At low temperatures, SMMs exhibit slow relaxation of their magnetization induced by a combined effect of their uni-axial anisotropy ($D_{ST} < 0$) and high-spin ground state (S_T). These two characteristics create an energy barrier (Δ_A), equal to $|D_{ST}|S_T^2$ for integer spins and $|D_{ST}|(S_T^2 - 1/4)$ for half-integer spins, between the two thermodynamically

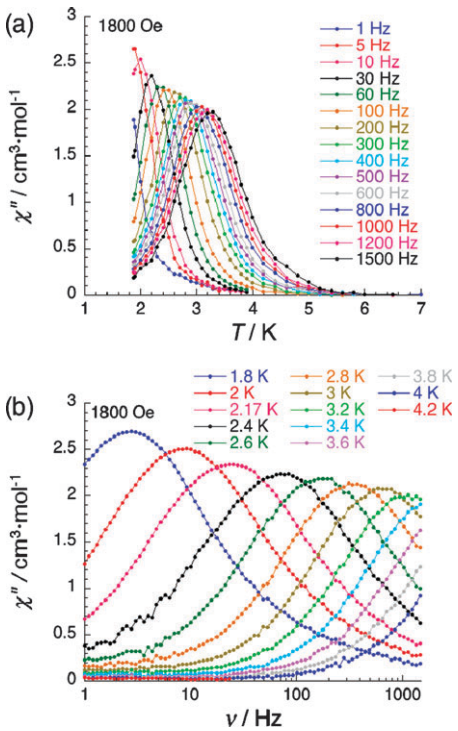

Fig. 11 Temperature dependence at different ac frequencies (a) and frequency dependence at different temperatures (b) of the out-of-phase component of the ac susceptibility for **3** below 7 K under 1800 Oe.

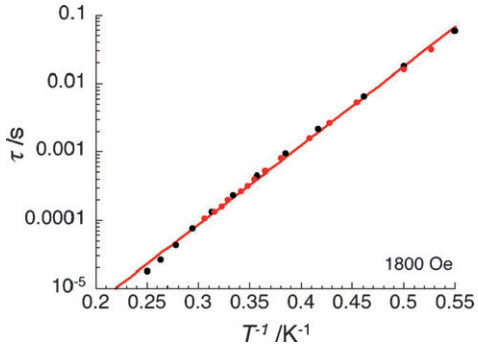

Fig. 12 Plot of the relaxation time τ *vs.* $1/T$ for **3** under 1800 Oe. Red dots are the relaxation times deduced from the temperature dependence of the out-of-phase component of the ac susceptibility at different ac frequencies. Black dots are the relaxation times deduced from the frequency dependence of the out-of-phase component of the ac susceptibility at different temperatures. The red solid line is the best fit obtained with an Arrhenius law.

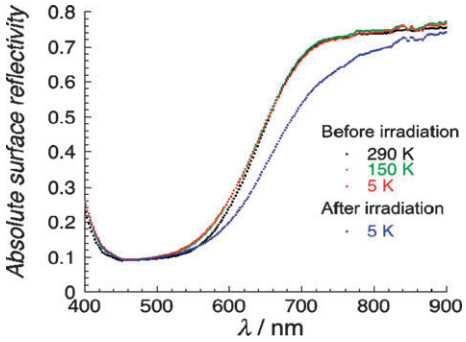

Fig. 13 Absolute surface reflectivity *vs.* wavelength for $Na_2[Fe(CN)_5NO]\cdot 2H_2O$ at different temperatures measured under a white light of 0.5 mW cm^{-2}. At 5 K, the red and blue dots are respectively before and after irradiation at 470 nm (60 mW cm^{-2}).

equivalent spin configurations $m_S = \pm S_T$. These theoretical considerations, taking $\Delta_A = \Delta_{eff}$, make possible an estimation of the magnetic anisotropy of the spin ground state, D_{ST} at about −1.7 K. Remarkably, almost identical values of D_{ST} and thus Δ_A, are found for related $[Mn_2(SB)_2]^{2+}$ complexes in $[Mn_2(saltmen)_2(ReO_4)_2]$[26a] or $[Mn_2(salpn)_2(H_2O)_2](ClO_4)_2$ (with $salpn^{2-}$ = *N*,*N*′-1,3-propylenebis(salicylideneiminato) anion).[26b] It is worth noting that the value of D_{ST} implies a local Mn^{III} anisotropy, D_{Mn}/k_B, of −3.8 K[22,26] that is almost four times the value deduced from our approximated model but is perfectly in agreement with previous estimations.[22,26] This result confirms that the magnetic parameters deduced from the approximated models of the magnetic susceptibility (*vide supra*) must be taken with caution.

The magnetic properties of **3** have been studied in great details using dc and ac techniques but the role of the magnetic interactions (likely of antiferromagnetic nature based on the magnetic properties of **1** and **2**) between $[Mn_2(saltmen)_2]^{2+}$ cations through the diamagnetic [NC–$(Fe(CN)_3NO)$–CN] links, seems to be quite different on the static and dynamic properties. While the dc susceptibility suggests a significant effect of these interactions as shown by the only qualitative analyses obtained from our simplified magnetic models, the dynamics of the magnetization is almost identical to isolated $[Mn_2(SB)_2]^{2+}$ SMMs[26a] supporting the negligible influence of the inter-$[Mn_2(saltmen)_2]^{2+}$ couplings. Indeed these results might be correlated to the peculiar 2D square organization of the dinuclear Mn^{III} units (Fig. 6) as already observed in 2D networks of SMMs.[30] Clearly, the complete understanding of the effects of the magnetic interactions between $[Mn_2(saltmen)_2]^{2+}$ cations on the static and dynamic properties of **3** still needs further theoretical work beyond the subject of this paper.

Optical properties

Optical properties of compounds **1–3** have also been studied using solid-state reflectivity measurements. As an introduction to these measurements, the photochromic properties of the $Na_2[Fe(CN)_5NO]\cdot 2H_2O$ precursor have been first explored studying the thermal dependence of the reflectivity spectra (on a powder sample) using a low power white light (0.5 mW cm^{-2}).

The spectrum remains almost unchanged when the temperature decreases from room temperature down to 5 K (Fig. 13). In order to probe the photoactivity of the precursor at 5 K, an irradiation with a 470 nm blue light (60 mW cm^{-2}) was performed during 10 min; it is worth noting that longer irradiation times do not change the photoinduced spectrum shown in Fig. 13. A significant decrease in the reflectivity is observed above 560 nm. This result is in agreement with previous optical data measured in transmission mode on crystals of $Na_2[Fe(CN)_5NO]$,[19a,31] that showed the appearance of new bands in the 600–800 nm region predominantly associated with a photoinduced metal–ligand charge transfer from the Fe^{II} metal ion to the nitrosyl ligand to form Fe^{III}–$NO^{\bullet}$ pairs.[19,32]

After this blue light excitation, the compound was warmed up with a temperature sweeping-rate of 6 K min^{-1}. The reflectivity spectra changes increasing the temperature, and the initial spectrum before irradiation is recovered around 220 K. To illustrate this thermal behavior, the reflectivity can be plotted at a given wavelength as a function of the temperature as shown at 740 nm in Fig. 14. Before irradiation, the reflectivity at 740 nm is almost constant when the temperature is lowered, in agreement with the very small dependence of the spectra with temperature. During the 470 nm irradiation, the

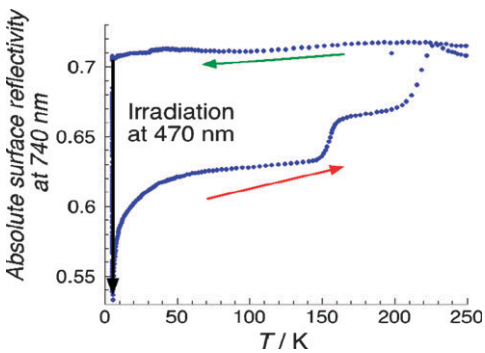

Fig. 14 Absolute surface reflectivity at 740 nm *vs.* the temperature for the $Na_2[Fe(CN)_5NO]\cdot 2H_2O$ precursor: green arrow: cooling mode before irradiation, black arrow: irradiation at 470 nm (at 60 mW cm^{-2}), red arrow: heating mode after irradiation.

reflectivity decreases with a very fast dynamics from 0.72 to 0.53. When the irradiation is stopped, the reflectivity starts to increase rapidly with the increase of the temperature and two marked steps appear at 155 and 220 K. This peculiar thermal behavior, that has been well summarized in ref. 19*a*, involves three different metastable phases. The low-temperature increase below 50 K is attributed to a relaxation from the photo-induced Fe^{II}–$NO^{\bullet}$ state to both Fe^{II}–ON and Fe^{II}-(η^2-NO) configurations in the SI and SII states, respectively. At 155 K, the Fe^{II}–ON SI state converts into the Fe^{II}–NO ground state, while the relaxation of the Fe^{II}-(η^2-NO) SII state is observed only at 220 K.[19] The surface reflectivity technique is thus an efficient tool to study in detail the photochromic properties of the $Na_2[Fe(CN)_5NO]\cdot 2H_2O$ precursor, and similar experiments were therefore carried out for the three new materials based on $[Mn(SB)]^+$ and $[Fe(CN)_5NO]^{2-}$ building blocks.

The performed measurements indicate that the optical spectra of these compounds changed in the red and 700–900 nm domains when the temperature decreases from room temperature down to 5 K (Fig. S10–S12, ESI†). These changes are associated to the thermal dependence of the optical spectra of $[Mn(SB)]^+$ cations as shown by the measurements performed on the Mn/SB precursors. When the compounds **1**, **2** and **3** are irradiated at 5 K by a 470 nm blue light, the spectra remain almost unmodified before and after irradiation (Fig. S13–S15, ESI†). Therefore none of these new compounds display photochromic properties induced by the presence of the $[Fe(CN)_5NO]^{2-}$ anions. Indeed, these results are in agreement with those obtained on similar compounds incorporating $[Mn(SB)]^+$ and $[Fe(CN)_5NO]^{2-}$ moieties,[19*d*] for which the authors concluded that the photoinduced metastable states are not observed when the cyanido groups are coordinating with Mn^{III} metal ions. Additional experiments have been performed on compounds **1–3** comparing the magnetic susceptibilities before and after *in situ* irradiation at 10 K. No photomagnetic effect has been observed as judged by the magnetic response that stays unchanged independently of the used wavelength of irradiation.

Conclusion

In this report, three new materials based on $[Fe(CN)_5NO]^{2-}$ and $[Mn(SB)]^+$ building blocks have been synthesized and structurally characterized: a trinuclear $[Mn(5\text{-Br-salpn})(H_2O)]_2[Fe(CN)_5NO]\cdot 2H_2O$ complex **1**, and two 2D coordination networks: $[\{Mn(salen)\}_2Fe(CN)_5NO]\cdot 2H_2O$ (**2**) and $[\{Mn(saltmen)\}_4Fe(CN)_5NO](ClO_4)_2\cdot H_2O\cdot 2CH_3OH$ (**3**). While the magnetic properties of **1** and **2** reveal weak antiferromagnetic interaction between $S = 2$ $[Mn(SB)]^+$ units *via* NC–Fe–CN links, **3** present slow relaxation of its magnetization at low temperatures. This dynamic behavior is indeed almost identical to isolated $[Mn_2(SB)_2]^{2+}$ SMMs even though the static susceptibility seems to be influenced by the weak coupling through the $[Fe(CN)_5NO]^{2-}$ bridges. Further theoretical work beyond the scope of the present report will be necessary to explain consistently the static and dynamic properties of this material probably in relation with its two-dimensional network. The photochromism of the $Na_2[Fe(CN)_5NO]\cdot 2H_2O$ precursor has been studied by reflectivity measurements that agree well with other optical techniques used previously. Unfortunately, similar experiments on compound **1–3** indicate that the $[Fe(CN)_5NO]^{2-}$ motif does not bring photochromic or photomagnetic properties to these new materials.

Experimental

Synthesis

All chemicals and solvents used in these syntheses were of reagent grade. The precursors, $[Mn(saltmen)(H_2O)](ClO_4)$, $[Mn(salen)(H_2O)](ClO_4)$, $[Mn(5\text{-Br-salpn})(H_2O)](ClO_4)$ ($saltmen^{2-}$ = *N*,*N*′-(1,1,2,2-tetramethylethylene) bis(salicylideneiminato) dianion, $salen^{2-}$ = *N*,*N*′-ethylenebis(salicylideneiminato) dianion, 5-Br-salpn^{2-} = *N*,*N*′-1,3-propylenebis(5-bromo-salicylideneiminato) dianion) was prepared according to literature procedures.[22,26] **Caution:** perchlorate salts of metal complexes with organic ligands are potentially explosive. Only small amounts of the material should be prepared and it should be handled with extreme care.

$[Mn(5\text{-Br-salpn})(H_2O)]_2[Fe(CN)_5NO]\cdot 2H_2O$ (1). A mixture of $[Mn^{III}(5\text{-Br-salpn})(H_2O)](ClO_4)$ (1 eq., 0.2 mmol) in 10 ml methanol was mixed with $Na_2[Fe(CN)_5NO]\cdot 2H_2O$ (1 eq., 0.2 mmol) in 2 ml H_2O. After stirring for 30 min. the resulting dark brown solution was filtered. The filtrate was left undisturbed at room temperature to produce thin lamellar brown single crystals suitable for X-ray diffraction within 4 days. Yield: in *ca.* 15% based on Mn. Anal. calc. for $C_{39}H_{36}Br_4FeMn_2N_{10}O_9$ (1274.15 g mol^{-1}): C, 36.77; H, 2.85; N, 10.99. Found: C, 36.58; H, 2.50; N, 10.86%. IR (KBr) data/cm^{-1}: ν(C≡N) 2145.4, 2155.9, ν(N≡O) 1908.6, 1941.6, ν(C=N) 1613.7.

$[\{Mn(salen)\}_2Fe(CN)_5NO]\cdot 2H_2O$ (2). The procedure was the same as for **1** except that $[Mn^{III}(5\text{-Br-salpn})(H_2O)](ClO_4)$ was replaced by $[Mn(salen)(H_2O)](ClO_4)$ (1 eq., 0.2 mmol). Yield: 45% based on Mn. Anal. calc. for $C_{37}H_{28}FeMn_2N_{10}O_6$ (874.42 g mol^{-1}): C, 50.82; H, 3.23; N, 16.02. Found: C, 50.90; H, 3.50; N, 15.82%. IR (KBr) data/cm^{-1}: ν(C≡N) 2147.9, ν(N≡O) 1922.0, ν(C=N) 1629.0.

$[\{Mn(saltmen)\}_4Fe(CN)_5NO](ClO_4)_2\cdot 2CH_3OH\cdot H_2O$ (3). The procedure was the same as for **1** except that $[Mn(salen)(H_2O)](ClO_4)$ was replaced by $[Mn(saltmen)(H_2O)](ClO_4)$ (1 eq., 0.2 mmol). Yield: 60% based on Mn. Anal. calc. for $C_{87}H_{98}Cl_2FeMn_4N_{14}O_{20}$ (2006.30 g mol^{-1}): C, 52.08; H, 4.92; N, 9.77. Found: C, 51.80; H, 4.50; N, 9.62. IR (KBr) data: ν(C≡N) 2154.6, ν(N≡O) 1931.7, ν(C=N) 1601.4, $\nu(ClO_4)$ 1085.5.

Physical methods

Elemental analysis for C, H and N were performed following the classical Pregl-Dumas technique on a ThermoFischer Flash EA1112.

FTIR spectra were recorded in the range of 400–4000 cm^{-1} on a Nicolet 750 Magna-IR spectrometer using KBr pellets.

Magnetic susceptibility measurements were obtained with the use of a Quantum Design SQUID magnetometer

(MPMS-XL). dc Measurements were conducted from 1.8 to 300 K and between −70 and 70 kOe applied dc fields. The measurements were performed on polycrystalline samples. Experimental data were corrected for the sample holder and for the diamagnetic contribution of the sample.

The optical studies have been performed with a home built reflectivity system. The temperature range is from 4.2 to 300 K. The spectrometric range runs from 400–900 nm. The used spectrometer is a high sensitivity Hamamatsu 10083CA. The spectra are measured with a Leica CLS 150 XD tungsten halogen source that was set at low power (0.5 mW/cm^2) onto the sample. The spectra are compared to a white reference obtained with a NIST traceable standard for reflectance (sphere Optics, ref SG3054). The background, which is the spectrum acquired with the light source switched off, is subtracted from all measurements. The reflectivity can be plotted either as a function of temperature, time or wavelength. To measure the photochromic effect at low temperature, we use a second source of irradiation with a LED Lumileds Luxeon V at 470 (±25) nm (60 mW cm^{-2}). Spectra after light irradiation are then obtained when the LED is switched off again.

X-Ray crystallographic data of complexes **1** and **2** were collected on a Nonius Kappa CCD diffractometer with graphite-monochromated Mo-Kα radiation (λ = 0.71073 Å) at 150(2) K. A suitable crystal was affixed on a glass fiber using silicone grease and transferred to the goniostat. DENZO-SMN[33] was used for data integration and SCALEPACK[33] corrected data for Lorentz-polarisation effects. The structures were solved by direct methods and refined by a full-matrix least-squares method on F^2 using the SHELXTL crystallographic software package.[34] During the refinement, all the non-H atoms were refined anisotropically except the disordered solvent water molecules in complex **1**. The H atoms on C atoms were included in calculated positions, whereas H atoms on O_{water} atoms were found from the residual peaks and refined with fixed isotropic thermal parameters based on those of parent atoms.

X-Ray crystallographic data of complex **3** were collected on station 11.3.1 of the Advanced Light Source at Lawrence Berkeley National Laboratory, from synchrotron radiation at 0.7749 Å, from a silicon 111 monochromator, using a Bruker Apex II CCD diffractometer. The structure was solved with and refined over F^2 with SHELXTL.[35] All non-hydrogens were refined anisotropically. The perchlorate ions occupy two crystallographic sites with half occupancy. One of them presents a disorder over two positions of its oxygen atoms. These were refined with geometrical and displacement parameters restrains. Two methanol molecules with half occupancy sit close to one of the two perchlorates. These proximity and positional disorder result in unreal bond distances. Hydrogens were placed geometrically and refined with a riding model except those of the water and methanol molecules, that are missing in this structural model. Small voids remain in the structure that contain only very diffuse electron density peaks. Use of PLATON/SQUEEZE to take these into account did not improve significantly the quality of the structure, and therefore it was left out.

Selected bond lengths and angles of **1–3** are listed in Tables 1–3, respectively. The detailed crystal data and structure refinement for **1–3** are given in Table 4.

Acknowledgements

This work was supported by the CNRS, the University of Bordeaux, MAGMANet (NMP3-CT-2005-515767), the GDR MCM (Magnétisme et Commutation Moléculaires) and the Conseil Régional d'Aquitaine. R. C. and X. L. thank the Chinese Scholarship Council for the funding of the scientific stay of X. L. at the CRPP. We also acknowledge the provision of time at the ALS synchrotron facility with financial support from the U.S. Department of Energy (Contract DE-AC02-05CH11231). The authors wish to thank Prof. Hitoshi Miyasaka and Dr. Nigel Hearns for the fruitful discussions that helped us in this work.

References

1 (*a*) P. D. W. Boyd, Q. Li, J. B. Vincent, K. Folting, H.-R. Chang, W. E. Streib, J. C. Huffman, G. Christou and D. N. Hendrickson, *J. Am. Chem. Soc.*, 1988, **110**, 8537; (*b*) A. Caneschi, D. Gatteschi and R. Sessoli, *J. Am. Chem. Soc.*, 1991, **113**, 5873; (*c*) R. Sessoli, H.-L. Tsai, A. R. Schake, S. Wang, J. B. Vincent, K. Folting, D. Gatteschi, G. Christou and D. N. Hendrickson, *J. Am. Chem. Soc.*, 1993, **115**, 1804; (*d*) D. Gatteschi, R. Sessoli and J. Villain, *Molecular Nanomagnets*, Oxford University Press, Oxford, UK, 2006.

2 (*a*) A. Caneschi, D. Gatteschi, N. Lalioti, C. Sangregorio, R. Sessoli, G. Venturi, A. Vindigni, A. Rettori, M. G. Pini and M. A. Novak, *Angew. Chem., Int. Ed.*, 2001, **40**, 1760; (*b*) R. Clérac, H. Miyasaka, M. Yamashita and C. Coulon, *J. Am. Chem. Soc.*, 2002, **124**, 12837; (*c*) H. Miyasaka and R. Clérac, *Bull. Chem. Soc. Jpn.*, 2005, **78**, 1725; (*d*) C. Coulon, H. Miyasaka and R. Clérac, *Struct. Bonding*, 2006, **122**, 163; (*e*) H. Miyasaka, M. Julve, M. Yamashita and R. Clérac, *Inorg. Chem.*, 2009, **48**, 3420.

3 (*a*) M. N. Leuenberger and D. Loss, *Nature*, 2001, **410**, 789; (*b*) W. Wernsdorfer, N. Aliaga-Alcalde, D. N. Hendrickson and G. Christou, *Nature*, 2002, **416**, 406; (*c*) F. Troiani, A. Ghirri, M. Affronte, S. Carretta, P. Santini, G. Amoretti, S. Piligkos, G. Timco and R. E. P. Winpenny, *Phys. Rev. Lett.*, 2005, **94**, 207208; (*d*) F. Troiani, M. Affronte, S. Carretta, P. Santini and G. Amoretti, *Phys. Rev. Lett.*, 2005, **94**, 190501; (*e*) J. Lehmann, A. Gaita-Arino, E. Coronado and D. Loss, *Nature Nanotech.*, 2007, **2**, 312; (*f*) L. Bogani and W. Wernsdorfer, *Nat. Mater.*, 2008, **7**, 179; (*g*) D. Stepanenko, M. Trif and D. Loss, *Inorg. Chim. Acta*, 2008, **361**, 3740.

4 (*a*) D. Gatteschi and R. Sessoli, *Angew. Chem., Int. Ed.*, 2003, **42**, 268; (*b*) J. Long, in *Chemistry of Nanostructured Materials*, ed. P. Yang, World Scientific Publishing, Hong Kong, 2003, p. 291; (*c*) E. Brechin, *Chem. Commun.*, 2005, 5141; (*d*) A. Cornia, A. Fabretti Costantino, L. Zobbi, A. Caneschi, D. Gatteschi, M. Mannini and R. Sessoli, *Struct. Bonding*, 2006, **122**, 133; (*e*) G. Aromí and E. K. Brechin, *Struct. Bonding*, 2006, **122**, 1; (*f*) J. N. Rebilly and T. Mallah, *Struct. Bonding*, 2006, **122**, 103.

5 (*a*) H. Miyasaka, R. Clérac, K. Mizushima, K. Sugiara, M. Yamashita, W. Wernsdorfer and C. Coulon, *Inorg. Chem.*, 2003, **42**, 8203; (*b*) T. Liu, D. Fu, S. Gao, Y. Zhang, H. Sun, G. Su and Y. Liu, *J. Am. Chem. Soc.*, 2003, **125**, 13976; (*c*) N. Shaikh, A. Panja, S. Goswami, P. Banerjee, P. Vojtısek, Y.-Z. Zhang, G. Su and S. Gao, *Inorg. Chem.*, 2004, **43**, 849; (*d*) N. E. Chakov, W. Wernsdorfer, K. A. Abboud and G. Christou, *Inorg. Chem.*, 2004, **43**, 5919; (*e*) S. Wang, J. L. Zuo, S. Gao, Y. Song, H. C. Zhou, Y. Z. Zhang and X. Z. You, *J. Am. Chem. Soc.*, 2004, **126**, 8900; (*f*) E. Pardo, R. Ruiz-Garcia, F. Lloret, J. Faus, M. Julve, Y. Journaux, F. S. Delgado and C. Ruiz-Pérez, *Adv. Mater.*, 2004, **16**, 1597; (*g*) T. Kajiwara, M. Nakano, Y. Kaneko, S. Takaishi, T. Ito, M. Yamashita, A. Igashira-Kamiyama,

H. Nojiri, Y. Ono and N. Kojima, *J. Am. Chem. Soc.*, 2005, **127**, 10150; (*h*) L. Bogani, C. Sangregorio, R. Sessoli and D. Gatteschi, *Angew. Chem., Int. Ed.*, 2005, **44**, 5817; (*i*) Z.-M. Sun, A. V. Prosvirin, H.-H. Zhao, J.-G. Mao and K. R. Dunbar, *J. Appl. Phys.*, 2005, **97**, 10B305; (*j*) H. Miyasaka, T. Nezu, K. Sugimoto, K. Sugiura, M. Yamashita and R. Clérac, *Chem.–Eur. J.*, 2005, **11**, 1592; (*k*) Y.-L. Bai, J. Tao, W. Wernsdorfer, O. Sato, R.-B. Huang and L.-S. Zheng, *J. Am. Chem. Soc.*, 2006, **128**, 16428; (*l*) K. Bernot, L. Bogani, A. Caneschi, D. Gatteschi and R. Sessoli, *J. Am. Chem. Soc.*, 2006, **128**, 7947; (*m*) Y.-Z. Zheng, M.-L. Tong, W.-M. Zhang and X.-M. Chen, *Angew. Chem., Int. Ed.*, 2006, **45**, 6310; (*n*) X.-N. Cheng, W.-X. Zhang, Y.-Z. Zheng and X.-M. Chen, *Chem. Commun.*, 2006, 3603; (*o*) H. Z. He, Z.-L. Wang, S. Gao and C.-H. Yan, *Inorg. Chem.*, 2006, **45**, 6694; (*p*) N. Ishii, T. Ishida and T. Nogami, *Inorg. Chem.*, 2006, **45**, 3837; (*q*) H. Miyasaka, T. Madanbashi, K. Sugimoto, Y. Nakazawa, W. Wernsdorfer, K. Sugiura, M. Yamashita, C. Coulon and R. Clérac, *Chem.–Eur. J.*, 2006, **12**, 7028; (*r*) X.-M. Zhang, Z.-M. Hao, W.-X. Zhang and X.-M. Chen, *Angew. Chem., Int. Ed.*, 2007, **46**, 3456; (*s*) J. T. Brockman, T. C. Stamatatos, W. Wernsdorfer, K. A. Abboud and G. Christou, *Inorg. Chem.*, 2007, **46**, 9160; (*t*) K. Bernot, L. Bogani, R. Sessoli and D. Gatteschi, *Inorg. Chim. Acta*, 2007, **360**, 3807; (*u*) H. Tanaka, T. Kajiwara, Y. Kaneko, S. Takaishi and M. Yamashita, *Polyhedron*, 2007, **26**, 2105; (*v*) A. Saitoh, H. Miyasaka, M. Yamashita and R. Clérac, *J. Mater. Chem.*, 2007, **17**, 2002; (*w*) E. Pardo, R. Ruiz-Garcia, F. Lloret, J. Faus, M. Julve, Y. Journaux, M. A. Novak, F. S. Delgado and C. Ruiz-Pérez, *Chem.–Eur. J.*, 2007, **13**, 2054; (*x*) H.-B. Xu, B.-W. Wang, F. Pan, Z.-M. Wang and S. Gao, *Angew. Chem., Int. Ed.*, 2007, **46**, 7388; (*y*) Y.-Z. Zheng, W. Xue, M.-L. Tong, X.-M. Chen and S.-L. Zheng, *Inorg. Chem.*, 2008, **47**, 11202; (*z*) K. Bernot, J. Luzon, R. Sessoli, A. Vindigni, J. Thion, S. Richeter, D. Leclercq, J. Larionova and A. van der Lee, *J. Am. Chem. Soc.*, 2008, **130**, 1619; (*aa*) Th. C. Stamatatos, K. A. Abboud, W. Wernsdorfer and G. Christou, *Inorg. Chem.*, 2009, **48**, 807; (*ab*) E. Coronado, J. R. Galan-Mascaros and C. Martí-Gastaldo, *J. Am. Chem. Soc.*, 2008, **130**, 14987; (*ac*) K. S. Gavrilenko, O. Cador, K. Bernot, P. Rosa, R. Sessoli, S. Golhen, V. V. Pavlishchuk and L. Ouahab, *Chem.–Eur. J.*, 2008, **14**, 2034; (*ad*) Y.-G. Huang, X.-T. Wang, F.-L. Jiang, S. Gao, M.-Y. Wu, Q. Gao, W. Wei and M.-C. Hong, *Chem.–Eur. J.*, 2008, **14**, 10340; (*ae*) A. V. Palii, O. S. Reu, S. M. Ostrovsky, S. I. Klokishner, B. S. Tsukerblat, Z.-M. Sun, J.-G. Mao, A. V. Prosvirin, H.-H. Zhao and K. R. Dunbar, *J. Am. Chem. Soc.*, 2008, **130**, 14729; (*af*) S. W. Przybylak, F. Tuna, S. J. Teat and R. E. P. Winpenny, *Chem. Commun.*, 2008, 1983; (*ag*) Y.-Z. Zheng, W. Xue, M.-L. Tong, X.-M. Chen, F. Grandjean and G. J. Long, *Inorg. Chem.*, 2008, **47**, 4077; (*ah*) H. Miyasaka, A. Saitoh, M. Yamashita and R. Clérac, *Dalton Trans.*, 2008, 2422.

6 (*a*) R. Lescouëzec, J. Vaissermann, C. Ruiz-Pérez, F. Lloret, R. Carrasco, M. Julve, M. Verdaguer, Y. Dromzee, D. Gatteschi and W. Wernsdorfer, *Angew. Chem., Int. Ed.*, 2003, **42**, 1483; (*b*) L. M. Toma, F. S. Delgado, C. Ruiz-Pérez, R. Carrasco, J. Cano, F. Lloret and M. Julve, *Dalton Trans.*, 2004, 2836; (*c*) L. M. Toma, R. Lescouëzec, F. Lloret, M. Julve, J. Vaissermann and M. Verdaguer, *Chem. Commun.*, 2003, 1850; (*d*) R. Lescouëzec, L. M. Toma, J. Vaissermann, M. Verdaguer, F. S. Delgado, C. Ruiz-Pérez, F. Lloret and M. Julve, *Coord. Chem. Rev.*, 2005, **249**, 2691; (*e*) M. Ferbinteanu, H. Miyasaka, W. Wernsdorfer, K. Nakata, K. Sugiura, M. Yamashita, C. Coulon and R. Clérac, *J. Am. Chem. Soc.*, 2005, **127**, 3090; (*f*) L. M. Toma, R. Lescoüezec, J. Pasan, C. Ruiz-Pérez, J. Vaissermann, J. Cano, R. Carrasco, W. Wernsdorfer, F. Lloret and M. Julve, *J. Am. Chem. Soc.*, 2006, **128**, 4842; (*g*) H.-R. Wen, C.-F. Wang, Y. Song, S. Gao, J.-L. Zuo and X.-Z. You, *Inorg. Chem.*, 2006, **45**, 8942; (*h*) L. M. Toma, R. Lescoüezec, S. Uriel, R. Llusar, C. Ruiz-Pérez, J. Vaissermann, F. Lloret and M. Julve, *Dalton Trans.*, 2007, 3690; (*i*) S. W. Choi, H. Y. Kwak, J. H. Yoon, H. C. Kim, E. K. Koh and C. S. Hong, *Inorg. Chem.*, 2008, **47**, 10214.

7 R. E. P. Winpenny, *J. Chem. Soc., Dalton Trans.*, 2002, 1.

8 (*a*) W. R. Entley and G. S. Girolami, *Science*, 1995, **268**, 397; (*b*) S. Ferlay, T. Mallah, R. Ouahès, P. Veillet and M. Verdaguer, *Nature*, 1995, **378**, 701; (*c*) S. M. Holmes and G. S. Girolami, *J. Am. Chem. Soc.*, 1999, **121**, 5593; (*d*) H. Miyasaka, N. Matsumoto, H. Okawa, N. Re, R. Crescenzi and C. Floriani, *J. Am. Chem. Soc.*, 1996, **118**, 981; (*e*) T. E. Vos and J. S. Miller, *Angew. Chem., Int. Ed.*, 2005, **44**, 2416; (*f*) M. Verdaguer, A. Bleuzen, V. Marvaud, J. Vaissermann, M. Seuleiman, C. Desplanches, A. Scuiller, C. Train, R. Garde, G. Gelly, C. Lomenech, I. Rosenman, P. Veillet, C. C. Cartier dit Moulin and F. Villain, *Coord. Chem. Rev.*, 1999, **190–192**, 1023; (*g*) B. Sieklucka, R. Podgajny, T. Korzeniak, P. Przychodzen and R. Kania, *C. R. Chim.*, 2002, **50**, 639.

9 (*a*) L. M. Beltran and J. R. Long, *Acc. Chem. Res.*, 2005, **38**, 325; (*b*) C. P. Berlinguette, D. Vaughn, C. Canada-Vilalta, J. R. Galán-Mascarós and K. R. Dunbar, *Angew. Chem., Int. Ed.*, 2003, **42**, 1523; (*c*) T. Glaser, M. Heidemeier, T. Weyhermüller, R.-D. Hoffmann, H. Rupp and P. Müller, *Angew. Chem., Int. Ed.*, 2006, **45**, 6033; (*d*) S. Wang, J.-L. Zuo, H.-C. Zhou, H. J. Choi, Y. Ke, J. R. Long and X.-Z. You, *Angew. Chem., Int. Ed.*, 2004, **43**, 5940; (*e*) D. F. Li, S. Parkin, G. Wang, G. T. Yee, A. V. Prosvirin and S. M. Holmes, *Inorg. Chem.*, 2005, **44**, 4903; (*f*) E. J. Schelter, A. V. Prosvirin and K. R. Dunbar, *J. Am. Chem. Soc.*, 2004, **126**, 15004; (*g*) A. V. Palii, S. M. Ostrovsky, S. I. Klokishner, B. S. Tsukertlat, C. P. Berlinguette, K. R. Dunbar and J. R. Galán-Mascarós, *J. Am. Chem. Soc.*, 2004, **126**, 16860; (*h*) Y. Song, P. Zhang, X.-M. Ren, X.-F. Shen, Y.-Z. Li and X.-Z. You, *J. Am. Chem. Soc.*, 2005, **127**, 3708.

10 (*a*) H. Oshio, H. Onodera, O. Tamada, H. Mizutanu, T. Hikichi and T. Ito, *Chem.–Eur. J.*, 2000, **6**, 2523; (*b*) S. Bonhommeau, G. Molnár, A. Galet, A. Zwick, J.-A. Real, J. J. McGarvey and A. Bousseksou, *Angew. Chem., Int. Ed.*, 2005, **44**, 406; (*c*) C. P. Berlinguette, A. Dragulescu-Andrasi, A. Sieber, H.-U. Güdel, C. Achim and K. R. Dunbar, *J. Am. Chem. Soc.*, 2005, **127**, 6766; (*d*) W. Kosaka, K. Nomura, K. Hashimoto and S.-i. Ohkoshi, *J. Am. Chem. Soc.*, 2005, **127**, 8590.

11 (*a*) O. Sato, T. Iyoda, A. Fujishima and K. Hashimoto, *Science*, 1996, **272**, 704; (*b*) A. Goujon, O. Roubeau, F. Varret, A. Dolbecq, A. Bleuzen and M. Verdaguer, *Eur. Phys. J. B*, 2000, **14**, 115; (*c*) O. Sato, T. Kawakami, M. Kimura, S. Hishiya, S. Kubo and Y. Einaga, *J. Am. Chem. Soc.*, 2004, **126**, 13176; (*d*) V. Escax, G. Champion, M.-A. Arrio, M. Zacchigna, C. Cartier and A. Bleuzen, *Angew. Chem., Int. Ed.*, 2005, **44**, 4798; (*e*) O. Sato, Y. Einaga, A. Fujishita and K. Hashimoto, *Inorg. Chem.*, 1999, **38**, 4405; (*f*) S.-i. Ohkoshi, H. Tokoro, T. Hozumi, Y. Zhang, K. Hashimoto, C. Mathonière, I. Bord, G. Rombaut, M. Verelst, C. Cartier-dit-Moulin and F. Villain, *J. Am. Chem. Soc.*, 2006, **128**, 270; (*g*) S.-i. Ohkoshi, S. Ikeda, T. Hozumi, Kashiwagi and T. Hashimoto, *J. Am. Chem. Soc.*, 2006, **128**, 5320; (*h*) J.-M. Herrera, V. Marvaud, M. Verdaguer, J. Marrot, M. Kalisz and C. Mathonière, *Angew. Chem., Int. Ed.*, 2004, **43**, 5648.

12 (*a*) H. J. Choi, J. J. Sokol and J. R. Long, *J. Phys. Chem. Solids*, 2004, **65**, 839; (*b*) H. J. Choi, J. J. Sokol and J. R. Long, *Inorg. Chem.*, 2004, **43**, 1606; (*c*) S. F. Si, J. K. Tang, Z. Q. Liu, D. Z. Liao, Z. H. Jiang, S. P. Yan and P. Cheng, *Inorg. Chem. Commun.*, 2003, **6**, 1109; (*d*) H. Miyasaka, H. Takahashi, T. Madanbashi, K.-I. Sugiura, R. Clérac and H. Nojiri, *Inorg. Chem.*, 2005, **43**, 5969; (*e*) X. Shen, B. Li, J. Zou, H. Hu, Y. Yu and S. Liu, *Transition Met. Chem.*, 2002, **27**, 372; (*f*) X. Shen, B. Li, J. Zou, H. Hu and Z. Xu, *J. Mol. Struct.*, 2003, **657**, 325.

13 (*a*) N. Re, E. Gallo, C. Floriani, H. Miyasaka and N. Matsumoto, *Inorg. Chem.*, 1996, **35**, 6004; (*b*) H.-R. Wen, C.-F. Wang, Y.-Z. Li, J.-L. Zuo and X.-Z. You, *Inorg. Chem.*, 2006, **45**, 7032.

14 (*a*) H. Miyasaka, N. Matsumoto, N. Re, E. Gallo and C. Floriani, *Inorg. Chem.*, 1997, **36**, 670; (*b*) H. Miyasaka, H. Ieda, N. Matsumoto, N. Re, R. Crescenzi and C. Floriani, *Inorg. Chem.*, 1998, **37**, 2741; (*c*) H. Miyasaka, H. Ieda, N. Matsumoto, N. Re, R. Crescenzi and C. Floriani, *Inorg. Chem.*, 2003, **42**, 3509; (*d*) H. Miyasaka, H. Ieda, N. Matsumoto, N. Re, R. Crescenzi and C. Floriani, *Inorg. Chem.*, 1997, **36**, 670–676; (*e*) H. Miyasaka, H. Okawa, A. Miyazaka and T. Enoki, *Inorg. Chem.*, 1998, **37**, 4878.

15 (*a*) N. Matsumoto, Y. Sunatsuki, H. Miyasaka, Y. Hashimoto, D. Luneau and J.-P. Tuchagues, *Angew. Chem., Int. Ed.*, 1999, **38**, 171; (*b*) Z.-H. Ni, H.-Z. Kou, L.-F. Zhang, C. Ge, A.-L. Cui,

R.-J. Wang, Y. Li and O. Sato, *Angew. Chem., Int. Ed.*, 2005, **44**, 7742; (*c*) P. Przychodzeń, K. Lewinski, M. Balanda, R. Pelka, M. Rams, T. Wasiutynshi, C. Guyard-Duhayon and B. Sieklucka, *Inorg. Chem.*, 2004, **8**, 2967; (*d*) P. Przychodzeń, M. Rams, C. Guyard-Duhayon and B. Sieklucka, *Inorg. Chem. Commun.*, 2005, **8**, 350; (*e*) H.-Z. Kou, Z.-H. Ni, B. C. Zhou and R.-J. Wang, *Inorg. Chem. Commun.*, 2004, **7**, 1150; (*f*) Y. Kim, S.-M. Park and S.-J. Kim, *Inorg. Chem. Commun.*, 2002, **5**, 592; (*g*) X. Liu, O. Roubeau and R. Clérac, *C. R. Chim.*, 2008, **11**, 1182.

16 (*a*) W.-W. Ni, Z.-H. Ni, A.-L. Cui, X. Liang and H.-Z. Kou, *Inorg. Chem.*, 2007, **46**, 22; (*b*) Z.-H. Ni, L. Zheng, L.-F. Zhang, A.-L. Cui, W.-W. Ni, C.-C. Zhao and H.-Z. Kou, *Eur. J. Inorg. Chem.*, 2007, **9**, 1240.

17 See for example a photomagnetic $[Co_4Fe_4]$ cube: D. Li, R. Clérac, O. Roubeau, E. Harté, C. Mathonière, R. Le Bris and S. M. Holmes, *J. Am. Chem. Soc.*, 2008, **130**, 252.

18 See for example, a SCO system: M. Nihei, M. Yokota, L. Han, A. Maeda, H. Kishida, H. Okamoto and H. Oshio, *Angew. Chem., Int. Ed.*, 2005, **44**, 6484.

19 (*a*) P. Gütlich, Y. Garcia and T. Woike, *Coord. Chem. Rev.*, 2001, **219–221**, 839; (*b*) Z.-Z. Gu, O. Sato, T. Iyoda, K. Hashimoto and A. Fujishima, *Chem. Mater.*, 1997, **9**, 1092; (*c*) F. Bellouard, M. Clemente-León, E. Coronado, J. R. Galán-Mascarós, C. Giménez-Saiz, C. J. Gómez-García and T. Woike, *Polyhedron*, 2001, **20**, 1615; (*d*) M. Clemente-Léon, E. Coronado, J. R. Galán-Mascarós, C. J. Gómez-García, T. Woike and J. M. Clemente-Juan, *Inorg. Chem.*, 2001, **40**, 87; (*e*) M. D. Carducci, M. R. Pressprich and P. Coppens, *J. Am. Chem. Soc.*, 1997, **119**, 2669; (*f*) D. Schaniel and T. Woike, *Phys. Rev. B: Condens. Matter Mater. Phys.*, 2005, **71**, 174112; (*g*) P. Coppens, I. Novozhilova and A. Kovalevsky, *Chem. Rev.*, 2002, **102**, 861.

20 (*a*) S. Kawata and Y. Kawata, *Chem. Rev.*, 2000, **100**, 1777; (*b*) L. Hesselink, S. S. Orlov and M. C. Bashaw, *Proc. IEEE*, 2004, **92**, 1231.

21 H. Miyasaka, A. Saitoh and S. Abe, *Coord. Chem. Rev.*, 2007, **251**, 2622.

22 H. Miyasaka, R. Clérac, T. Ishii, H.-C. Chang, S. Kitagawa and M. Yamashita, *J. Chem. Soc., Dalton Trans.*, 2002, 1528.

23 (*a*) H. L. Shyu, H. H. Wei and Y. Wang, *Inorg. Chim. Acta*, 1997, **258**, 81; (*b*) Z. N. Chen, J. L. Wang, J. Qiu, F. G. Miao and W. X. Tang, *Inorg. Chem.*, 1995, **34**, 2255.

24 C. J. O'Connor, *Prog. Inorg. Chem.*, 1982, **29**, 203.

25 (*a*) J. Curély, *Physica B*, 1998, **245**, 263; (*b*) J. Curély, *Physica B*, 1998, **254**, 277; (*c*) J. Curély and J. Rouch, *Physica B*, 1998, **254**, 298.

26 (*a*) H. Miyasaka, R. Clérac, W. Wernsdorfer, L. Lecren, C. Bonhomme, K. Sugiura and M. Yamashita, *Angew. Chem., Int. Ed.*, 2004, **43**, 2801; (*b*) L. Lecren, W. Wernsdorfer, Y.-G. Li, A. Vindigni, H. Miyasaka and R. Clérac, *J. Am. Chem. Soc.*, 2007, **129**, 5045.

27 In order to take into account the interactions between Mn(III) dinuclear units, the following definition of the susceptibility has been used:

$$\chi = \frac{\chi_{Mn2}}{1 - \frac{2zJ'}{Ng^2\mu_B^2}\chi_{Mn2}}$$

see for example: (*a*) B. E. Myers, L. Berger and S. Friedberg, *J. Appl. Phys.*, 1969, **40**, 1149; (*b*) C. J. O'Connor, *Prog. Inorg. Chem.*, 1982, **29**, 203.

28 From J' (the mean-field interaction between dinuclear units), the magnetic interaction between Mn(III) metal ions can be easily estimated as $J_{Mn-Mn} = J'{S_T}^2/{S_{Mn}}^2$ and thus with $z = 6$, $J_{Mn-Mn}/k_B = -0.002$ K.

29 J. J. Borrás-Almenar, J. M. Clemente-Juan, E. Coronado and B. S. Tsukerblat, *J. Comput. Chem.*, 2001, **22**, 985.

30 H. Miyasaka, K. Nakata, L. Lecren, C. Coulon, Y. Nakazawa, T. Fijisaki, K.-I. Sugiura, M. Yamashita and R. Clérac, *J. Am. Chem. Soc.*, 2006, **128**, 3770.

31 T. Woike, W. Krasser, P. S. Bechthold and S. Haussül, *Phys. Rev. Lett.*, 1984, **53**, 1767.

32 J. Tritt-Goc, N. Pislewski and S. K. Hoffmann, *Chem. Phys. Lett.*, 1997, **268**, 471.

33 Z. Otwinowski and W. Minor, *Methods Enzymol.*, 1996, **276**, 307.

34 (*a*) G. M. Sheldrick, *SHELXL97 Program for Crystal Structure Refinement*, University of Göttingen, Göttingen, Germany, 1997; (*b*) G. M. Sheldrick, *SHELXS97 Program for Crystal Structure Solution*, University of Göttingen, Göttingen, Germany, 1997.

35 G. M. Sheldrick, *SHELXTL: Bruker AXS*, Madison, WI, USA, 2001.

